Journal of
Marine Science and Engineering

MDPI

Article

Organic Carbon Oxidation in the Sediment of the Ulleung Basin in the East Sea

Jae Seong Lee [1,2,*], Sung-Han Kim [1,2], Ju-Wook Baek [1,2], Kyung-Tae Kim [1], Dongseon Kim [1,2], Young-il Kim [3], Won-Chan Lee [4], Sung-Uk An [1], Chang Hwan Kim [3], Chan Hong Park [3] and Sokjin Hong [4]

1 Marine Environment Research Center, Korea Institute of Ocean Science and Technology, 385, Haeyang-ro, Yeongdo-gu, Busan 49111, Korea; sunghan@kiost.ac.kr (S.-H.K.); baekjw@kiost.ac.kr (J.-W.B.); ktkim@kiost.ac.kr (K.-T.K.); dkim@kiost.ac.kr (D.K.); asuppl@kiost.ac.kr (S.-U.A.)
2 Department of Convergence Study on the Ocean Science and Technology, Ocean Science and Technology School, 385, Haeyang-ro, Yeungdo-gu, Busan 49111, Korea
3 Dokdo Research Center, East Sea Research Institute, Korea Institute of Ocean Science and Technology, 48, Haeyanggwahak-gil, Uljin 36315, Korea; yikim@kiost.ac.kr (Y.-i.K.); kimch@kiost.ac.kr (C.H.K.); chpark@kiost.ac.kr (C.H.P.)
4 Marine Environment Research Division, National Institute of Fisheries Science, 216, Gijanghaean-ro, Gijang-eup, Busan 46083, Korea; phdleewc@korea.kr (W.-C.L.); 71sj@korea.kr (S.H.)
* Correspondence: leejs@kiost.ac.kr

Abstract: We characterized the biogeochemical organic carbon (C_{org}) cycles in the surface sediment layer of the Ulleung Basin (UB) of the East Sea. The total oxygen uptake (TOU) rate and the diffusive oxygen uptake (DOU) rate of the sediment were measured using an autonomous in situ benthic lander equipped with a benthic chamber (KIOST Belc*II*) and a microprofiler (KIOST Belp*II*). The TOU rate was in the range of 1.51 to 1.93 mmol O_2 m^{-2} d^{-1}, about double the DOU rate. The high TOU/DOU ratio implies that the benthic biological activity in the upper sediment layer is one of the important factors controlling benthic remineralization. The in situ oxygen exposure time was about 20 days, which is comparable to the values of other continental margin sediments. The sedimentary C_{org} oxidation rates ranged from 6.4 to 6.5 g C m^{-2} yr^{-1}, which accounted for ~2% of the primary production in UB. The C_{org} burial fluxes ranged from 3.14 ± 0.12 to 3.48 ± 0.60 g C m^{-2} yr^{-1}, corresponding to more than 30% of the deposited C_{org} buried into the inactive sediment deep layer.

Keywords: benthic chamber; benthic nutrients flux; benthic organic carbon oxidation; East Sea; in situ measurement; oxygen microprofiler; sedimentary organic carbon; Ulleung Basin

check for updates

Citation: Lee, J.S.; Kim, S.-H.; Baek, J.-W.; Kim, K.-T.; Kim, D.; Kim, Y.-i.; Lee, W.-C.; An, S.-U.; Kim, C.H.; Park, C.H.; et al. Organic Carbon Oxidation in the Sediment of the Ulleung Basin in the East Sea. *J. Mar. Sci. Eng.* **2022**, *10*, 694. https://doi.org/10.3390/jmse10050694

Academic Editor: George Kontakiotis

Received: 13 April 2022
Accepted: 18 May 2022
Published: 19 May 2022

1. Introduction

The Ulleung Basin (UB) is located in the southern part of the East Sea (ES). The oligotrophic Tsushima warm current flows in through the narrow Korea Strait between Korea and Japan, and it separates into a couple of strong streams by physical and meteorological forces close to the ES mouth [1]. As the floating warm waters move in the surface layer to the north of the ES, the complicated oceanographic features (seasonal upwelling, eddies, and seasonal variation in mixed layer thickness) may enhance the primary production in the euphotic depth [2–8], and half of the particulate organic carbon (C_{org}) produced by primary production in the euphotic depth (<100 m) can be transported vertically to the deep-sea sediment [9]. Thus, the UB has been suggested as a 'hot spot' for biogeochemical cycles of C_{org}, not only in the water column but also in the sediment [5].

Oxygen, the most favorable oxidizer for C_{org} decomposition, is used as an electron acceptor for C_{org} degradation [10,11]. The by-products produced via C_{org} degradation in the porewater are reoxidized in the oxic zone of the sediment layer. Consequently, oxygen consumption in the sediment can be represented quantitatively and can thus be used as a proxy of the total benthic carbon mineralization [10,11]. The sediment oxygen uptake rate has been measured using an enclosure incubation method and/or O_2 microprofiling

methods. The total oxygen uptake rate (TOU) measured by enclosure incubation in the laboratory or in situ represents the sum of oxygen consumption by benthic biology activities and carbon oxidation, which can be estimated from the initial rate of oxygen decrease in the enclosing chamber. Otherwise, the O_2 microprofiling method measures the diffusive oxygen uptake rate (DOU) via the sediment–water interface (SWI) using the high spatial distribution of O_2 in the diffusive boundary layer (DBL) near SWI by an oxygen microsensor (sensor tip < 1 mm) [12,13].

It has been difficult to measure the reliable sediment oxygen uptake rate for the deep-sea sediment (>1 km) because of unknown artifacts present during the sampling treatments [11]. The alteration of physical factors such as temperature and pressure during sediment recovery may allow for increasing sediment oxygen uptake. In addition, the inhomogeneous fauna density in cores also gives a significant bias to the results. Therefore, the ex situ sediment oxygen consumptions may have an uncertainty for the deep-sea sediment [11].

The main purpose of this study was to understand the biogeochemical C_{org} in the sediment of the UB, the most productive basin in the ES. To achieve our purpose, we simultaneously measured the TOU and DOU using an autonomous in situ benthic lander to quantify the C_{org} oxidation in the sediment. The partitioning sedimentary organic carbon fluxes were assessed to build the mass budget of C_{org} in the UB.

2. Materials and Methods

2.1. Study Area

The ES was expanded by the back-arc basin spreading between the Asian continent and Japan Island, which is one of the deepest marginal seas and is composed of three major basins (Ulleung, Yamato, and Japan) in the northwest Pacific (Figure 1) [14]. Because of the bowl shape of ES, with a relatively small spatial scale, the steep topography at the shelf–slope system allows for the mass transport of the sediment into the basin interior [14–16]. The UB, located in the southern part of the ES, is the entrance of the warm surface water of the Tsushima current. Along the Korean peninsula, temporal upwelling and warm eddies have been observed, and these may be important elements of primary production in the photic zone of the southwestern part of the ES [2–8].

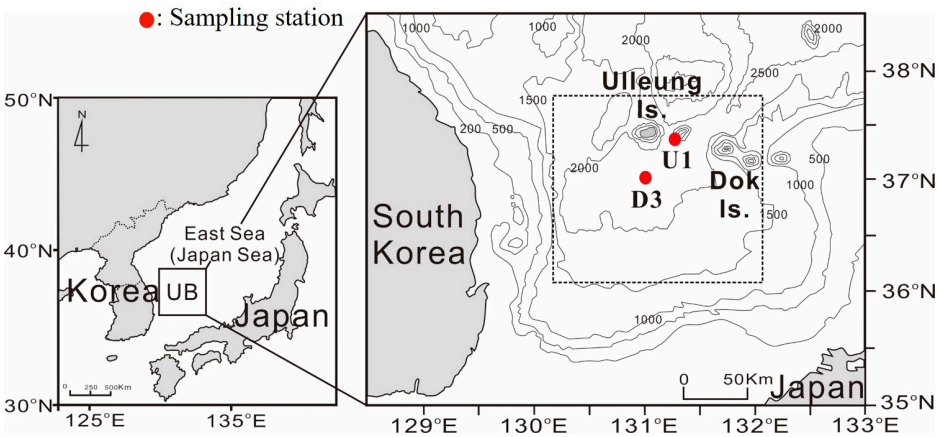

Figure 1. A map showing the sampling stations.

2.2. In Situ Measurement

The in situ measurements were carried out in September 2018 and April 2019 in the northern part of the UB (Figure 1, Table 1). The physical and biological parameters in the water column were measured before and after benthic deployment using CTD (SBE911Plus, Seabird Electronics Inc., Bellevue, WA, USA).

Table 1. Site location, water depth, temperature, salinity, and dissolved oxygen in bottom water.

	D3	U1
Latitude	37°00 N	37°24 N
Longitude	131°00 E	131°12 E
Water depth (m)	2154	2206
Bottom water salinity	34.07	34.06
Bottom water temperature (°C)	0.22	0.12
Bottom water DO (μmol L^{-1})	186	189

To measure the in situ sediment oxygen uptake rate (TOU and DOU), the autonomous benthic landers (KIOST Belc*II* and Belp*II*) were deployed. In brief, the benthic lander system was composed of a rectangular benthic chamber (Belc*II*) and miroprofiler (Belp*II*) [17–19]. The Belc*II* in situ incubation chamber was designed to measure the oxygen in the interior of the chamber to estimate the TOU. Additionally, the automatic water sampler can collect the incubated water samples in the chamber at preset time intervals to allow for benthic fluxes. Meanwhile, the Belp*II* consists of the four separate O_2 microoptode (Pyroscience, OXR50-HS-SUB & FSO2-SUBPORT, Aachen, Germany) systems and a custom-built motor-driven linear stage, allowing for the measurement of the high spatial distribution (<100 μm) of oxygen at the SWI [19].

Before the deployment of the benthic lander, we programmed each parameter for measurements into the microcontroller of the systems. The lander was deployed freely from a research vessel, and the distance from the ship to the system was continuously monitored using an acoustic pinger (Teledyne Benthos, 865-A) until touchdown. After finishing the in situ measurement (>24 h), the lander was ascended by releasing a weight. The incubated water samples of the Belc*II* were immediately filtered with 0.2 μm pore size filter paper (Milipore) and then stored in a deep freezer (−20 °C) until analysis in the laboratory [20].

2.3. Sediment Collection

To collect undisturbed sediment core samples, we carefully inserted a plexiglass tube (8 cm internal diameter, 40 cm long) into the sediment in the box corer. After sealing both ends of the core, it was temporarily stored in a refrigerator until core sectioning (<a few hours). The sediment core was sectioned at 1 cm intervals for measuring the C_{org} and the total nitrogen content (T-N) of the sediment and was stored in a deep freezer (<−20 °C) [18].

2.4. Laboratory Experiment

The in situ incubated water samples for nutrients were analyzed using a flow injection autoanalyzer (Bran+Luebbe, QuAAtro39 AutoAnalyzer) [20]. The water content of sediment was determined using weight loss after drying to a constant weight at 105 °C. The dry bulk density (DBD, g cm^{-3}) of sediment was calculated using the water content of the sediment and the grain density [18]. The dried sediment samples were acidified with 1 M HCl to measure the total C_{org} and nitrogen content of the sediment, and those were quantified by a CHN analyzer (Thermo Finnigan, Flash EA 1112, USA).

2.5. Flux Calculation

The benthic fluxes (TOU and nutrients) were estimated from a least-squares linear regression using the concentration gradients with the time and depth of the benthic chamber, as follows:

$$F_{TOU,\ BNF} = \left(\frac{dC}{dt}\right) \times \left(\frac{V}{A}\right) \quad (1)$$

where $F_{TOU,\ BNF}$ is the TOU and the benthic nutrient fluxes (mmol m^{-2} d^{-1}), dC/dt is the gradient of the linear regression line estimated from fitting the concentration (C) as a

function of the incubation time (t) (mmol m^{-3} d^{-1}), V is the chamber volume (m^3), and A is the chamber area (m^2) [17,18].

Using the high spatial resolution of the oxygen profiles, the upper DBL boundary and the sediment surface position were determined [12,13]. The upper DBL boundary was determined from the intersection of the constant oxygen concentration in the overlying water and the extrapolated linear oxygen gradient in the DBL. The sediment surface (z = 0) position was identified from a distinct change in the linear slope between the DBL and the porewater concentration. The oxygen penetration depth (OPD) was determined from the O_2 profiles as the depth where the signal of the O_2 microsensor reached a constant.

Using the high resolution of the vertical O_2 distributions, the DOUs and volumetric oxygen consumption rates were estimated by applying the numerical model PROFILE [21]. The two boundary conditions (BCs) in PROFILE were as follows: the first BC was the O_2 concentration at the sediment–water interface, and the second BC was that the flux at the bottom was zero. The apparent sediment molecular diffusion coefficient (D_s) was calculated with a diffusion coefficient of O_2 in the in situ temperature and sediment porosity [22,23].

The replicate the in situ measurements, OPD and DOU were compared using the nonparametric statistical Wilcoxon–Mann–Whitney test with a 95% confidence level. The statistical analysis was performed using the RStudio package.

2.6. C_{org} Budget Calculation

The C_{org} mass budget was calculated with following equation, assuming a steady state [24]:

$$C_{in} = C_{ox} + C_{burial} \quad (2)$$

where C_{in} is the input flux of C_{org} into the sediment from the water column, and C_{ox} is the oxidation flux of C_{org} that was determined by multiplying TOU and the Redfield ratio (106/138). The burial flux of C_{org} (C_{burial}) at the sediment layer was calculated with the following equation:

$$C_{burial} = C_{\infty} \times DBD \times SR \quad (3)$$

where C_{∞} is the mean C_{org} content (%) that shows the constant values of the lower layer (>30 cm), DBD is the mean DBD (g cm^{-3}) in the lower layer, and SR is the sedimentation rate of UB (0.06 cm yr^{-1}) [18].

3. Results

3.1. TOU and DOU

The TOU measurement at D3 in 2018 failed due to a failure of a microcontroller unit in Belc*II* (Figure 2). The TOU measured at U1 in September of 2018 was 1.51 mmol m^{-2} d^{-1}. With no significant spatial differences, the TOU values in 2019 were 1.89 and 1.93 mmol m^{-2} d^{-1} at D3 and U1, respectively (Table 2). However, the TOU values at U1 for 2019 were about 30% higher than those measured in September 2018. The result measured at D3 in April 2019 matched well the previous results of the same season [18].

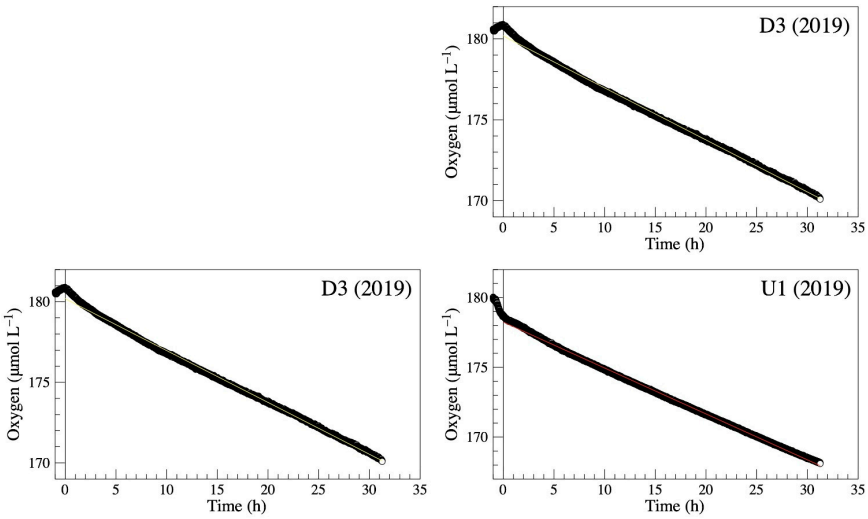

Figure 2. Variation of the concentration of O_2 with time during in situ incubation.

Table 2. The results of TOU, DOU, and benthic nutrient fluxes. The errors for TOU and BNF were calculated from the standard error for linear regression. The DOU errors represent the standard error for the duplicate measurements (n = 6).

		TOU	DOU	NH_4^+	NO_x^-	PO_4^{3-}	$Si(OH)_4$
				(mmol m^{-2} d^{-1})			
2018	D3	-	-	−0.09 ± 0.06 (R^2 = 0.21)	1.68 ± 0.54 (R^2 = 0.58)	0.09 ± 0.05 (R^2 = 0.32)	8.67± 2.18 (R^2 = 0.69)
	U1	1.52 ± 0.00	0.77 ± 0.13	−0.05 ± 0.07 (R^2 = 0.07)	0.29 ± 0.07 (R^2 = 0.78)	0.06 ± 0.03 (R^2 = 0.34)	1.08 ± 0.39 (R^2 = 0.6)
2019	D3	1.89 ± 0.00	-	−0.13 ± 0.07 (R^2 = 0.33)	1.41 ± 0.46 (R^2 = 0.61)	0.12 ± 0.04 (R^2 = 0.51)	6.98 ± 2.71 (R^2 = 0.45)
	U1	1.93 ± 0.00	1.00 ± 0.15	0.3 ± 0.04 (R^2 = 0.88)	−0.16 ± 0.07 (R^2 = 0.51)	0.01 ± 0.0 (R^2 = 0.57)	2.23 ± 0.25 (R^2 = 0.93)

The temporal variation of the O_2 microprofiles at U1 in the autumn and spring were not statistically significant for OPD (p = 0.125) and DOU (p = 0.25), which yielded 11.7 ± 0.4 mm for 2018, 12.4 ± 0.5 mm for 2019, 0.77 ± 0.13 mmol m^{-2} d^{-1} for 2018, and 1.00 ± 0.15 mmol m^{-2} d^{-1} for 2019 (Figure 3). The ratios of DOU and TOU were about 0.5, which was comparable to other deep-water depth results [11]. The volume-specific oxygen consumption rate (OCR) was divided into three layers in the oxic layer. In 2019, the OCR value in the upper surface sediment (up to 22.8 mm: 0.0029 nmol cm^{-3} s^{-1}) was higher by a factor of 1.75 than in 2018 (up to 28.5 mm: 0.0017 nmol cm^{-3} s^{-1}), which was similar to TOU—i.e., the sediment oxygen consumption was higher in April than in September, which may show a seasonal variation.

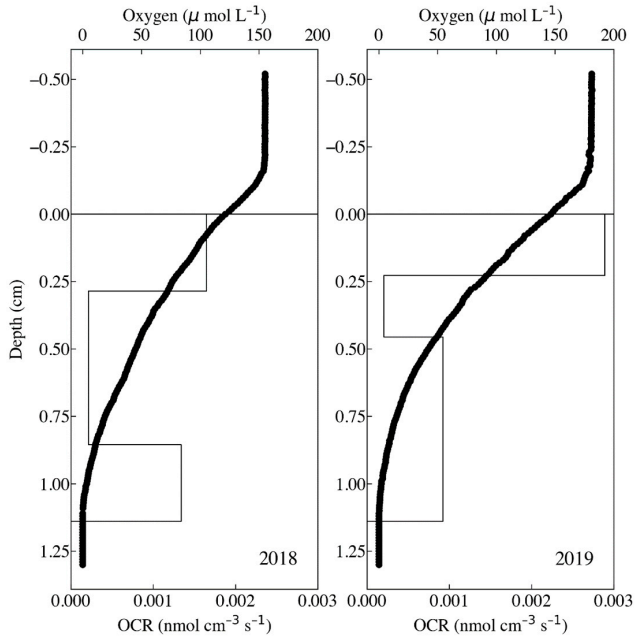

Figure 3. Examples of in situ vertical profiles of O_2 measured at U1 in 2018 and 2019 (solid circles). The line represents the volumetric oxygen consumption rate (OCR) calculated by Berg's model [21].

3.2. Benthic Nutrient Flux

The evolution of nutrients (ammonium, nitrate, phosphate, and silicate) with time generally shows organic matter degradation in the surface sediment (Figure 4). From the linear relationship of nutrient concentration with time, the benthic nutrient fluxes (BNFs) were estimated and are listed in Table 2. Overall, the nutrients gradually increased with time, but the ammonium and phosphate suggested poor linear regression results ($R^2 < 0.4$). This result may be explained ad the incubation times (22 h) for the estimation of ammonium flux, which seems to be insufficient for concentration buildup in the chamber. The ammonium, nitrate, phosphate, and silicate benthic fluxes ranged from -0.05 ± 0.07 to 0.30 ± 0.04, -0.16 ± 0.07 to 1.68 ± 0.54, 0.01 ± 0.00 to 0.12 ± 0.04, and 1.08 ± 0.39 to 8.67 ± 2.18 mmol m^{-2} d^{-1}, respectively. These results were comparable to previous in situ measurement results [18].

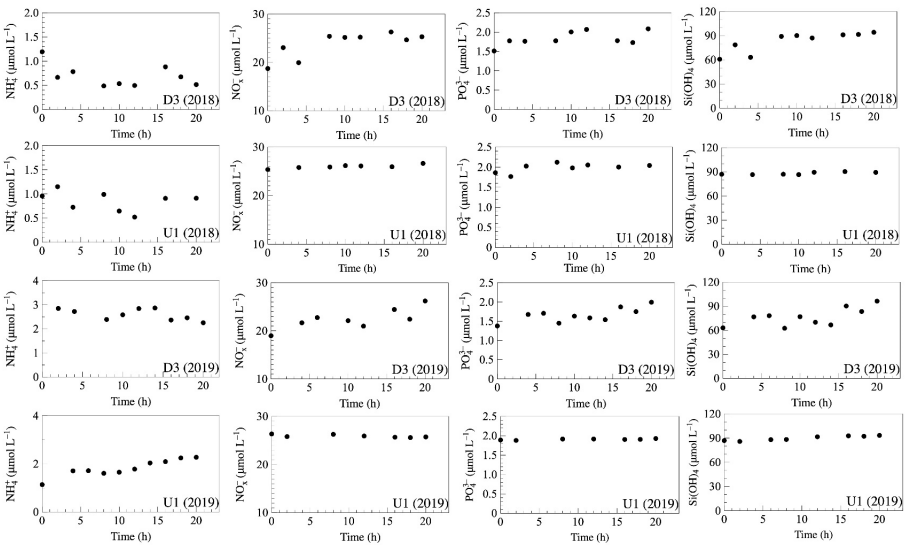

Figure 4. Evolution of ammonium, sum of nitrate (nitrate and nitrite), phosphate, and silicate concentrations during in situ incubation.

3.3. Vertical Distribution of C_{org} and Total Nitrogen Content

The C_{org} and T-N in the surface sediment (z = 0) at D3 and U1 were in the range of 2.53% to 2.73% and 0.33% to 0.36%, respectively (Figure 5). They were vertically decreased to ~10 cm sediment depth, and then both reached a constant content below 20 cm. The mean contents of C_{org} and T-N of the upper sediment layer (<10 cm) at U1 were 15% higher than at D3 (p = 0.002). However, the mean values of those below 20 cm of sediment depth were not statistically significant (p = 0.21). The same result was obtained for T-N, i.e., the upper surface T-N content at U1 was significantly higher than at D1, but below 20 cm of sediment depth. The results did not differ at both sites. The results for the sediment C_{org} and T-N were similar to previous results [20,25,26].

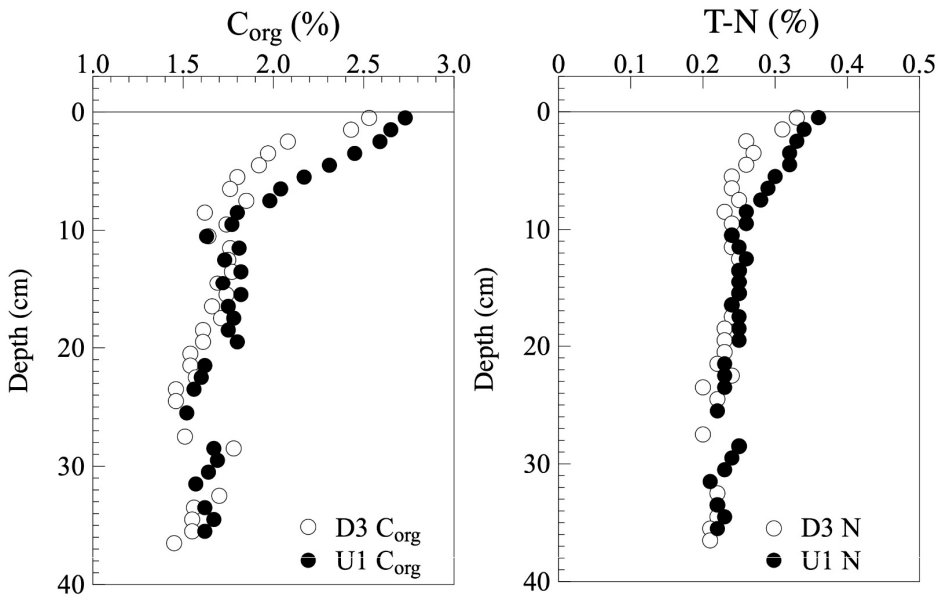

Figure 5. Vertical distribution of C_{org} and T-N of the sediment in 2018. The open circles represent the D3 station, and the solid circles represent the U1 station.

4. Discussion

The primary production (PP) in the UB ranged from 273 to 280 g C m^{-2} yr^{-1}, which was higher than that of the Kuroshio current region [8,27]. The higher export C_{org} fluxes from the euphotic zone may be expected, because the benthic remineralization in the sediment of the UB can be significantly higher than other deep-sea sediments [9]. Indeed, the C_{org} content and the significantly higher rate of anaerobic respirations (NO_x^-, Mn^{2+}, SO_4^{2-}) in the surface sediment layer of UB compared with other deep-sea sediments have suggested that the biogeochemical cycles of C_{org} and its anaerobic degradation pathways are important factors controlling the biogeochemical cycles of C_{org} [9,18].

4.1. Benthic C_{org} Oxidation in UB

The sediment oxygen uptake rate (TOU and DOU) has been widely used as a substitute for the C_{org} oxidation rate because it can represent the electron acceptors for total OM degradation [10,11,28]. The TOU, measured by the benthic chamber, normally represents the sum of the total remineralization rate of organic matter (OM), assuming that the O_2 in the incubated water is ultimately the consumption by OM oxidation, the reoxidation of reduced materials, and the benthic animal activities [11]. The DOU represents the oxygen uptake across the SWI followed by the concentration gradient between the water and sediment porewater, which is controlled mainly by the diffusion [10,11]. Therefore, the DOU may exclude the oxygen uptake mediated by benthic animal activities. The difference between the TOU and DOU (the fauna mediated oxygen uptake rate, FOU = TOU−DOU) is significant in the coastal sediment, where there is a higher biomass of benthic animals, which can account for about 50% of the TOU [11]. The depth attenuation of the FOU can

be explained by the distribution of biomass with water depth and the shift in the benthic animal feeding type from very active irrigating specimens to a less active deposit-feeder according to the sediment carbon content [11]. By contrast, it is less important at more than 1000 m water depth sediment because of the relatively low benthic fauna biomass. Note that our FOU was higher than for other deep-sea sediments, which implies that the respiration of benthos and the reoxidation of reduced materials by bioirrigation and biological mixing could contribute to the TOU. Indeed, the volumetric OCRs in the oxic–anoxic interface were comparable with the upper oxic layer (Figure 3). Our results suggest that the high reoxidation of the reduced elements (i.e., NH_4^+, Mn^{2+}, Fe^{2+}, and H_2S) at the oxic-anoxic interface can be enhanced by biological activities (bioirrigation and biological mixing), and thus, the thick Mn-oxide enrichment layer at the surface sediment of UB may be coupled with the cycles of Mn-oxide trapping via Mn^{2+} reoxidation. Consequently, these oxygen dynamics in the sediment layer can be an important step for controlling the reduced elements via organic matter oxidation pathways [9–11].

4.2. Benthic C_{org} Oxidation in UB

The partitioning C_{org} fluxes (C_{ox}, C_{burial}, and C_{in}) and burial efficiency (BE) are listed in Table 3. Assuming a steady state, the C_{org} oxidation will follow Redfield's stoichiometric relationship between C and O_2. The benthic C_{org} oxidation rate (C_{ox}) at the sediment of the UB ranged from 5.1 to 6.5 g C m^{-2} yr^{-1}, which was similar to previous results [18]. The C_{ox} at D3 and U1 were 6.61 and 6.36 g C m^{-2} yr^{-1}, respectively, which corresponded to about 2% of the primary production in the southwestern part of the ES. The C_{burial} at D3 and U1 were given as 3.48 ± 0.60 and 3.14 ± 0.12 g C m^{-2} yr^{-1}, respectively, which did not differ spatially and matched previous results well [18]. The C_{burial} fluxes accounted for ~1% of the annual mean primary production of the UB. Given that, at the UB, all deposited C_{org} is oxidized and buried into the sediment layer, the sedimentary C_{org} input fluxes (C_{in} = C_{ox} + C_{burial}) were 9.99 ± 0.60 and 9.51 ± 0.12 g C m^{-2} yr^{-1}, respectively, which suggested that the benthic cycles of C_{org} corresponded to about 3% of PP. The C_{org} budget across the slope to the basin suggests that the lateral transport C_{org} and the segregation of organic matter for those transports determine their fate [18]. At the deep interior, far away from the slope of the UB, the refractory organic matter could be progressively enriched following preferential degradation during lateral transport, and thus, the laterally transported C_{org} may contribute in a similar order to the vertical fluxes of C_{org}. This result suggests that the sediment of the UB can act as the burial place of C_{org} [18]. The burial efficiency of C_{org} in the sediment layer (BE = C_{burial}/C_{in} × 100) was about 34% at both stations, which was comparable with the other high productive marginal sea sediments [29–34].

Table 3. Organic carbon oxidation (C_{ox}), burial flux (C_{burial}), input flux (C_{in}), and burial efficiency (BE) in the sediment of the UB.

	C_{ox}	C_{burial}	C_{in}	BE
		(g C m^{-2} $year^{-1}$)		(%)
D3	6.51	3.48 ± 0.60	9.99 ± 0.60	34 ± 6
U1	6.36	3.14 ± 0.12	9.51 ± 0.12	33 ± 1

4.3. Oxygen Exposure Time (OET) in the UB

The in situ OET is the exposure time of C_{org} to oxygen at the location of deposition, which is important for understanding the mechanisms of C_{org} preservation in the sediment layer and/or the transport in the marginal sea [35,36]. We calculated the in situ OET at U1 by dividing the SR from the OPD (OET = OPD/SR), which were 20 ± 3 and 21 ± 4 y, which were similar to the California margin (1500–3500 m) and the Washington lower slope (600–2000 m) [35,36].

Kang et al. (2004) [37] reported that the O_2 concentration of the bottom water in the ES has decreased during the last century (1932–1996) with changes in the water mass structure. Given that the O_2 decrease in the bottom water will be progressing in the future, the OPD will be shallower, and thus, C_{org} preservation in the sediment will be more efficient. This implies that the sediment of the UB can act as the carbon reservoir and reactors. Our research is based on a fragmentary study, and a quantitative study on the biogeochemical cycles of the carbon-production-remineralization-transport-burial across from the slope to the basin system is needed to understand the function of the northeast Pacific margin sea in the global system.

5. Conclusions

In situ experiments and geochemical analyses were performed to understand the biogeochemical cycles of C_{org} in the benthic layer of the UB in the ES. The C_{org} oxidation rate of the sediment was consistent with previous results, which were relatively higher than other deep-sea sediments [18]. The high ratio of TOU/DOU suggests that the benthic biological activity in the surface sediment layer is an important factor for controlling the biogeochemical cycles of C_{org}. The large contribution of the O_2 consumption in the oxic–anoxic interface may be coupled with the Mn-oxide enrichment of the surface sediment layer. The relatively higher BE and OET compared to those of other marginal sea sediments suggests that the redistribution by lateral transport is one of the important keys in the biogeochemical cycles of C_{org} in the benthic boundary layer of the UB.

Author Contributions: Conceptualization, investigation, writing—original draft preparation, writing—review and editing, visualization, formal analysis, J.S.L.; investigation, methodology, J.-W.B.; formal analysis, writing—review and editing, S.-H.K.; writing—review and editing, K.-T.K.; funding acquisition, writing—review and editing, D.K.; investigation, methodology, Y.-i.K.; funding acquisition, writing—review and editing, W.-C.L.; writing—review and editing, S.-U.A.; formal analysis, C.H.K.; funding acquisition, C.H.P.; conceptualization, writing—review and editing, S.H. All authors have read and agreed to the published version of the manuscript.

Funding: This work was supported by the Korea Institute of Ocean Science and Technology (PEA0012), the Ministry of Oceans and Fisheries ("a sustainable research and development of Dokdo", PG52911), and the National Institute of Fisheries Science (R2022061).

Institutional Review Board Statement: Not applicable.

Informed Consent Statement: Not applicable.

Data Availability Statement: The data used to support the findings of this study are available from the corresponding author upon request.

Acknowledgments: We wish to thank the crews of the R/V EARDO for their assistance during the benthic lander deployment and sediment core sampling. The support from C. H. Park and W.-C. Lee was helpful and greatly appreciated. In addition, we also thank the two anonymous reviewers for their helpful comments that improved the early version of the MS.

Conflicts of Interest: The authors declare no conflict of interest.

References

1. Lee, D.-K.; Seung, Y.H.; Kim, Y.-B.; Kim, Y.H.; Shin, H.-R.; Shin, C.-W.; Chang, K.-I. Circulation. In *Oceanography of the East Sea (Japan Sea)*; Chang, K.-I., Zhang, C.-I., Park, C., Kang, D.-J., Ju, S.-J., Lee, S.-H., Eds.; Springer International Publishing: Cham, Switzerland, 2015; pp. 87–126.
2. Hyun, J.-H.; Kim, D.; Shin, C.-W.; Noh, J.-H.; Yang, E.-J.; Mok, J.-S.; Kim, S.H.; Kim, H.C.; Yoo, S. Enhanced phytoplankton and bacterioplankton pro-duction coupled to coastal upwelling and an anticyclonic eddy in the Ulleung basin, East Sea. *Aquat. Microb. Ecol.* **2009**, *54*, 45–54. [CrossRef]
3. Kim, D.; Yang, E.J.; Kim, K.H.; Shin, C.-W.; Park, J.; Yoo, S.; Hyun, J.-H. Impact of an anticyclonic eddy on the summer nutrient and chlorophyll *a* distribution in the Ulleung Basin, East Sea (Japan Sea). *ICES J. Mar. Sci.* **2012**, *69*, 23–29. [CrossRef]
4. Kwak, J.H.; Hwang, J.; Choy, E.J.; Park, H.J.; Kang, D.-J.; Lee, T.; Chang, K.-I.; Kim, K.-R.; Kang, C.-K. High primary production and f-ratio in summer in the Ulleung basin of the East/Japan Sea. *Deep Sea Res. Part I Oceanogr. Res. Pap.* **2013**, *79*, 74–85. [CrossRef]

5. Kwak, J.H.; Lee, S.H.; Park, H.J.; Choy, E.J.; Jeong, H.D.; Kim, K.R.; Kang, C.K. Monthly measured primary and new productivities in the Ulleung Basin as a biological "hot spot" in the East/Japan Sea. *Biogeosciences* **2013**, *10*, 4405–4417. [CrossRef]
6. Park, K.-A.; Ullman, D.S.; Kim, K.; Chung, Y.J.; Kim, K.-R. Spatial and temporal variability of satellite-observed subpolar front in the East/Japan Sea. *Deep Sea Res. Part I Oceanogr. Res. Pap.* **2007**, *54*, 453–470. [CrossRef]
7. Park, K.-A.; Woo, H.-J.; Ryu, J.-H. Spatial scales of mesoscale eddies from GOCI chlorophyll-*a* concentration images in the East/Japan Sea. *Ocean Sci. J.* **2012**, *47*, 347–358. [CrossRef]
8. Yoo, S.; Park, J. Why is the southwest the most productive region of the East Sea/Sea of Japan? *J. Mar. Syst.* **2009**, *78*, 301–315. [CrossRef]
9. Kim, D.; Choi, M.-S.; Oh, H.-Y.; Song, Y.-H.; Noh, J.-H.; Kim, K.H. Seasonal export fluxes of particulate organic carbon from234Th/238U disequilibrium measurements in the Ulleung Basin (Tsushima Basin) of the East Sea (Sea of Japan). *J. Oceanogr.* **2011**, *67*, 577–588. [CrossRef]
10. Canfield, D.E.; Kristensen, E.; Thamdrup, B. The Oxygen Cycle. In *Aquatic Geomicrobiology*; Canfield, D.E., Kristensen, E., Thamdrup, B., Eds.; Elsevier: New York, NY, USA, 2005; pp. 167–204. [CrossRef]
11. Glud, R.N. Oxygen dynamics of marine sediment. *Mar. Biol. Res.* **2008**, *4*, 243–289. [CrossRef]
12. Jørgensen, B.B.; Revsbech, N.P. Diffusive boundary layers and the oxygen uptake of sediments and detritus. *Limnol. Oceanogr.* **1985**, *30*, 111–122. [CrossRef]
13. Nøhr Glud, R.; Gundersen, J.K.; Revsbech, N.P.; Jørgensen, B.B. Effects on the benthic diffusive boundary layer imposed by microelectrodes. *Limnol. Oceanogr.* **1994**, *39*, 462–467. [CrossRef]
14. Lee, G.H.; Kim, H.J. Crustal structure and tectonic evolution of the East Sea. In *Oceanography of the East Sea (Japan Sea)*; Chang, K.-I., Zhang, C.-I., Park, C., Kang, D.-J., Ju, S.-J., Lee, S.-H., Eds.; Springer International Publishing: Cham, Switzerland, 2015; pp. 415–430.
15. Koo, B.-Y.; Kim, S.-P.; Lee, G.-S.; Chung, G.S. Seafloor morphology and surface sediment distribution of the Southwestern part of Ulleung Basin, East Sea. *JKESS* **2014**, *35*, 131–146. [CrossRef]
16. Lee, H.J.; Choug, S.K.; Yoon, S.H. Slope-stability change from late pleistocene to holocene in the Ulleung Basin, East Sea (Japan Sea). *Sediment. Geol.* **1996**, *104*, 39–51. [CrossRef]
17. Lee, J.S.; An, S.-U.; Park, Y.-G.; Kim, E.; Kim, D.; Kwon, J.N.; Kang, D.-J.; Noh, J.-H. Rates of total oxygen uptake of sediments and benthic nutrients fluxes measured using an in situ autonomous benthic chamber in the sediment of the slope off the southwestern part of Ulleung Basin, East Sea. *Ocean Sci. J.* **2015**, *50*, 581–588. [CrossRef]
18. Lee, J.S.; Han, J.H.; An, S.-U.; Kim, S.-H.; Lim, D.; Kim, D.; Kang, D.-J.; Park, Y.-G. Sedimentary organic carbon budget across the slope to the basin in the southwestern Ulleung (Tsushima) Basin of the East (Japan) Sea. *J. Geophys. Res. Biogeosci.* **2019**, *124*, 2804–2822. [CrossRef]
19. Lee, J.S.; Kim, E.-S.; Yoon, S.-H.; Cho, J.-H.; Bahk, K.-S.; Kang, D.-J. Development and application of a novel miniature in situ microprofiler (NAFRI Belp*I*). *Ocean Sci. J.* **2012**, *47*, 489–495. [CrossRef]
20. Hansen, P.H.; Koroleff, F. Determination of Nutrients. In *Methods of Seawater Analysis*; Grasshoff, K., Kremling, K., Ehrhardt, M., Eds.; Wiley–VCH: Weinheim, Germany, 1999; pp. 159–228. [CrossRef]
21. Berg, P.; Risgaard-Petersen, N.; Rysgaard, N. Interpretation of measured concentration profiles in sediment pore water. *Limnol. Oceanogr.* **1998**, *43*, 1500–1510. [CrossRef]
22. Broecker, W.S.; Peng, T.-H. Gas exchange rates between air and sea. *Tellus* **1974**, *26*, 21–35. [CrossRef]
23. Li, Y.-H.; Gregory, G. Diffusion of ions in sea water and in deep sea sediment. *Geochim. Cosmochim. Acta* **1974**, *38*, 703–714. [CrossRef]
24. Martens, C.S.; Klump, J.V. Biogeochemical cycling in an organic-rich coastal marine basin 4. An organic carbon budget for sediments dominated by sulfate reduction and methanogenesis. *Geochim. Cosmochim. Acta* **1984**, *48*, 1987–2004. [CrossRef]
25. Cha, H.J.; Lee, C.B.; Kim, B.S.; Cho, M.S.; Ruttenberg, K.C. Early diagenetic redistribution and burial of phosphorus in the sediments of the southwestern East Sea (Japan Sea). *Mar. Geol.* **2005**, *216*, 127–143. [CrossRef]
26. Hyun, J.-H.; Kim, S.-H.; Mok, J.-S.; Cho, H.; Lee, T.; Vandieken, V.; Thamdrup, B. Manganese and iron reduction dominate organic carbon oxidation in deep continental margin sediments of the Ulleung Basin, East Sea. *Biogeosciences* **2017**, *14*, 941–958. [CrossRef]
27. Kim, M.; Hwang, J.; Rho, T.; Lee, T.; Kang, D.-J.; Chang, K.-I.; Noh, S.; Joo, H.; Kwak, J.H.; Kang, C.-K.; et al. Biogeochemical properties of sinking particles in the south-western part of the East Sea (Japan Sea). *J. Mar. Syst.* **2017**, *167*, 33–42. [CrossRef]
28. Canfield, D.E. Organic matter oxidation in marine sediments. In *Interactions of C, N, P and S Biogeochemical Cycles and Global Change*; Wollast, R., Chou, L., Mackenzie, F., Eds.; Springer: New York, NY, USA, 1993; pp. 333–356. [CrossRef]
29. Henrichs, S.M.; Farrington, J.W. Peru upwelling region sediment near 15°S. 1. Remineralization and accumulation of organic matter. *Limnol. Oceanogr.* **1984**, *29*, 1–19. [CrossRef]
30. Betts, J.N.; Holland, H.D. The oxygen content of ocean bottom waters, the burial efficiency of organic carbon, and the regulation of atmospheric oxygen. *Palaeogeogr. Palaeoclimatol. Palaeoecol.* **1991**, *97*, 5–18. [CrossRef]
31. Müller, P.J.; Suess, E. Productivity, sedimentation rate, and sedimentary organic matter in the oceans—I. Organic carbon preservation. *Deep-Sea Res. I Oceanogr. Res.* **1979**, *26*, 1347–1362. [CrossRef]
32. Rabouille, C.; Caprais, J.C.; Lansard, B.; Crassous, P.; Dedieu, K.; Reyss, J.L.; Khripounoff, A. Organic matter budget in the southeast Atlantic continental margin close to the Congo Canyon: In situ measurements of sediment oxygen consumption. *Deep-Sea Res. II Top. Stud. Oceanogr.* **2009**, *56*, 2223–2238. [CrossRef]

33. Epping, E.; van der Zee, C.; Soetaert, K.; Helder, W. On the oxidation and burial of organic carbon in sediments of the Iberian margin and Nazaré Canyon (NE Atlantic). *Prog. Oceanogr.* **2002**, *52*, 399–431. [CrossRef]
34. van Weering, T.C.E.; de Stigter, H.C.; Boer, W.; de Hass, H. Recent sediment transport and accumulation on the NW Iberian margin. *Prog. Oceanogr.* **2002**, *52*, 349–371. [CrossRef]
35. Hartnett, H.E.; Keil, R.G.; Hedge, J.I.; Devol, A.H. Influence of oxygen exposure time on organic carbon preservation in continental margin sediments. *Nature* **1998**, *391*, 572–574. [CrossRef]
36. Keil, R.G.; Dickens, A.F.; Arnarson, T.; Nunn, B.L.; Devol, A.H. What is the oxygen exposure time of laterally transported organic matter along the Washington margin? *Mar. Chem.* **2004**, *92*, 157–165. [CrossRef]
37. Kang, D.-J.; Kim, J.-Y.; Lee, T.; Kim, K.-R. Will the East/Japan Sea become an anoxic sea in the next century? *Mar. Chem.* **2004**, *91*, 77–84. [CrossRef]